Electromagnetic and Piezoelectric Transducers

André Preumont and Bilal Mokrani
ULB, Active Structures Laboratory,
CP. 165-42, 50 Av. F.D. Roosevelt,
B-1050 Brussels, Belgium

Abstract This chapter analyzes the two most popular classes of transducers used in active vibration control: the electromagnetic transducer known as *voice coil*, and the piezoelectric transducer. The first part of the chapter discusses the theory of the transducers and the second part discusses some applications in structural control.

1 Introduction

Transducers are critical in active structures technology; they can play the role of actuator, sensor, or simply energy converter, depending on the application and the electrical connections. In many applications, the actuators are the most critical part of the system; however, the sensors become very important in precision engineering where sub-micron amplitudes must be detected. This chapter begins with a description of the voice coil transducer and its application to the proof-mass actuator and the geophone (absolute velocity sensor). The remaining of the chapter is devoted to the piezoelectric materials and the constitutive equations of a discrete piezoelectric transducer.

2 Voice coil transducer

A *voice coil* transducer is an energy transformer which converts electrical power into mechanical power and vice versa. The system consists of a permanent magnet (Fig.1) which produces a uniform magnetic flux density B normal to the gap, and a coil which is free to move axially within the gap. Let v be the velocity of the coil, f the external force acting to maintain the coil in equilibrium against the electromagnetic forces, e the voltage difference across the coil and i the current into the coil. In this ideal transducer,

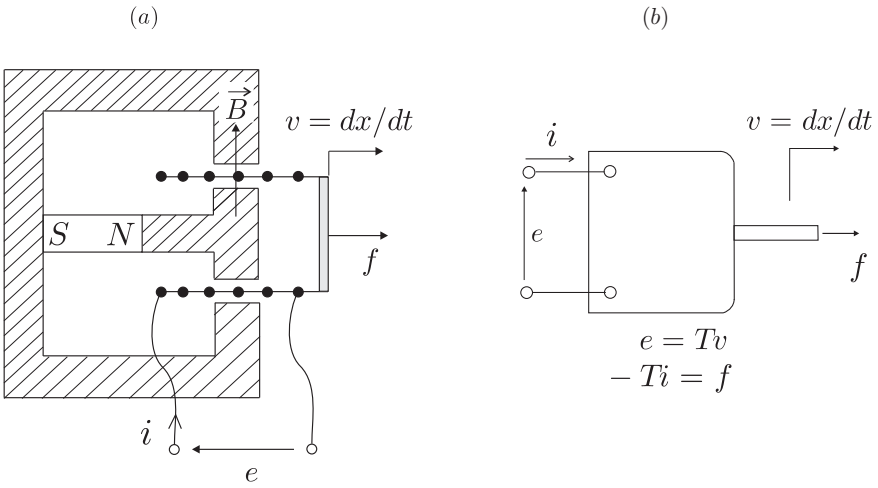

Figure 1. Voice-coil transducer: (a) Physical principle. (b) Symbolic representation.

we neglect the electrical resistance and the self inductance of the coil, as well as its mass and damping (if necessary, these can be handled by adding R and L to the electrical circuit of the coil, or a mass and damper to its mechanical model). The voice coil actuator is one of the most popular actuators in mechatronics (e.g. it is used in electromagnetic loudspeakers), but it is also used as sensor in geophones.

The first constitutive equation of the voice coil transducer follows from *Faraday's law*: A coil of n turns moving at the velocity v with respect to the magnetic flux density B generates an electromotive force (voltage) e given by

$$e = 2\pi nrBv = Tv \tag{1}$$

where

$$T = 2\pi nrB \tag{2}$$

is the *transducer constant*, equal to the product of the length of the coil exposed to the magnetic flux, $2\pi nr$, and the magnetic flux density B. The second equation follows from the L*orentz force* law: The external force f required to *balance* the total force of the magnetic field on n turns of the conductor is

$$f = -i\,2\pi nrB = -Ti \tag{3}$$

where i is the current intensity in the coil and T is again the transducer constant (2). Equation (1) and (3) are the constitutive equations of the voice coil transducer. Notice that the transducer constant T appearing in Faraday's law (1), expressed in $volt.sec/m$, is the same as that appearing in the Lorentz force (3), expressed in N/Amp.

The total power delivered to the moving-coil transducer is equal to the sum of the electric power, ei, and the mechanical power, fv. Combining with (1) and (3), one gets

$$ei + fv = Tvi - Tiv = 0 \tag{4}$$

Thus, at any time, there is an equilibrium between the electrical power absorbed by the device and the mechanical power delivered (and vice versa). The moving-coil transducer cannot store energy, and behaves as a perfect electromechanical converter. In practice, however, the transfer is never perfect due to eddy currents, flux leakage and magnetic hysteresis, leading to slightly different values of T in (1) and (3).

Let us now examine various applications of the voice coil transducer.

2.1 Proof-mass actuator

A proof-mass actuator (Fig.2) is an inertial actuator which is used in various applications of vibration control. A reaction mass m is connected to the support structure by a spring k, a damper c and a force actuator f which can be either magnetic or hydraulic. In the electromagnetic actuator discussed here, the force actuator consists of a voice coil transducer of constant T excited by a current generator i; the spring is achieved with membranes which also guide the linear motion of the moving mass. The system is readily modelled as in Fig.2.a. Combining the equation of a single d.o.f. oscillator with the Lorentz force law (3), one finds

$$m\ddot{x} + c\dot{x} + kx = Ti \tag{5}$$

or, in the Laplace domain,

$$x = \frac{Ti}{ms^2 + cs + k} \tag{6}$$

(s is the Laplace variable). The total force applied to the support is equal and opposite to the force applied to the proof-mass, $-m\ddot{x}$, or in Laplace form:

$$F = -ms^2x = \frac{-ms^2Ti}{ms^2 + cs + k} \tag{7}$$

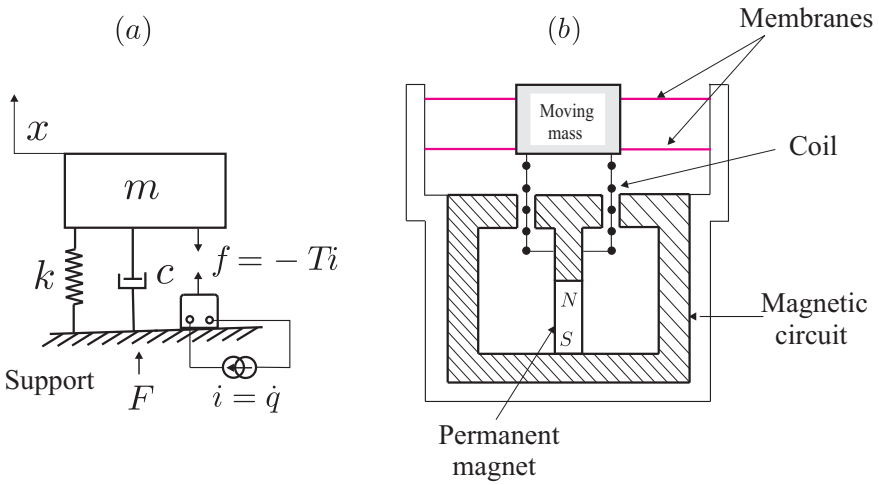

Figure 2. Proof-mass actuator (a) model assuming a current generator; (b) conceptual design of an electrodynamic actuator based on a voice coil transducer. The mass is guided by the membranes.

It follows that the transfer function between the total force F and the current i applied to the coil is

$$\frac{F}{i} = \frac{-s^2 T}{s^2 + 2\xi_p \omega_p s + \omega_p^2} \tag{8}$$

where T is the transducer constant (in N/Amp), $\omega_p = (k/m)^{1/2}$ is the natural frequency of the spring-mass system and ξ_p is the damping ratio, which in practice is fairly high, typically 20 % or more [the negative sign in (8) is irrelevant.] The Bode plots of (8) are shown in Fig.3; one sees that the system behaves like a high-pass filter with a high frequency asymptote equal to the transducer constant T; above some critical frequency $\omega_c \simeq 2\omega_p$, the proof-mass actuator can be regarded as an *ideal force generator*. It has no authority over the rigid body modes (at zero frequency) and the operation at low frequency requires a large stroke, which is technically difficult. Medium to high frequency actuators (40 Hz and more) are relatively easy to obtain with low cost components (loudspeaker technology).

If the current source is replaced by a voltage source (Fig.4), the modeling is slightly more complicated and combines the mechanical equation (5) and

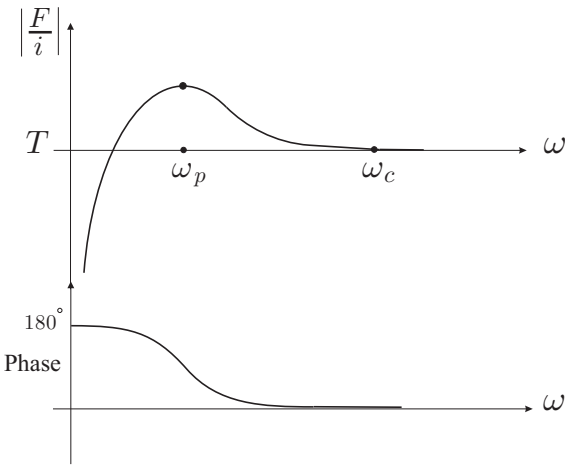

Figure 3. Bode plot F/i of an electrodynamic proof-mass actuator (amplitude and phase).

an electrical equation which is readily derived from Faraday's law:

$$T\dot{x} + L\frac{di}{dt} + Ri = E(t) \tag{9}$$

where L is the inductance R is the resistance of the electrical circuit and $E(t)$ is the external voltage source applied to the transducer.

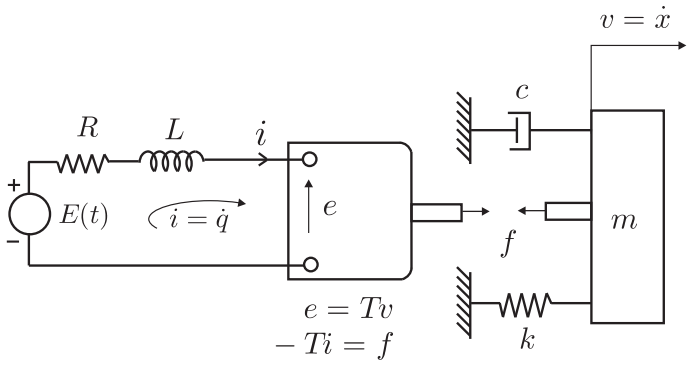

Figure 4. Model of a proof-mass actuator with a voltage source.

2.2 Geophone

The geophone is a transducer which behaves like an *absolute velocity sensor* above some cut-off frequency which depends on its mechanical construction. The system of Fig.2.a is readily transformed into a geophone by using the voltage e as the sensor output (Fig.5). If x_0 is the displacement of the support and if the voice coil is open ($i = 0$), the governing equations are

$$m\ddot{x} + c(\dot{x} - \dot{x}_0) + k(x - x_0) = 0$$

$$T(\dot{x} - \dot{x}_0) = e$$

combining these equations, one readily finds that

$$x - x_0 = \frac{-ms^2 x_0}{ms^2 + cs + k}$$

$$e = Ts(x - x_0) = \frac{-s^2 T}{s^2 + (c/m)s + k/m}\ sx_0$$

$$\frac{e}{\dot{x}_0} = \frac{-s^2 T}{s^2 + 2\xi_p \omega_p s + \omega_p^2} \tag{10}$$

Thus, there is a perfect *duality* between a proof-mass actuator and the geophone. The same device may be used either as actuator or sensor, depending on the electrical boundary conditions. The proof-mass actuator uses a current source while the geophone is connected to an infinite resistor.

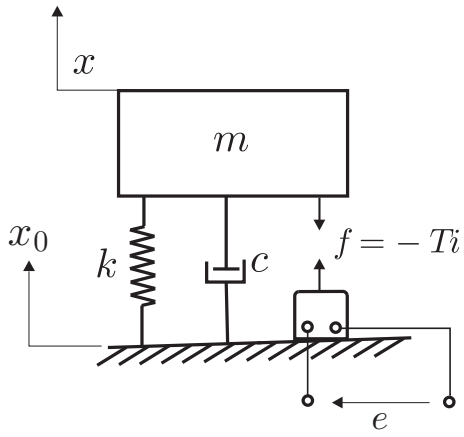

Figure 5. Model of a geophone based on a voice coil transducer.

Above the corner frequency, the gain of the geophone is equal to the transducer constant T. Designing geophones with very low corner frequency is in general difficult, especially if their orientation with respect to the gravity vector is variable; active geophones where the corner frequency is lowered electronically may constitute a good alternative option.

3 General electromechanical transducer

3.1 Constitutive equations

The constitutive behavior of a wide class of electromechanical transducers can be modeled as in Fig.6, where the central box represents the conversion mechanism between electrical energy and mechanical energy, and vice versa. In Laplace form, the constitutive equations read

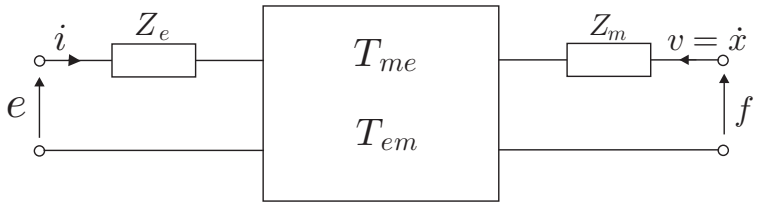

Figure 6. Electrical analog representation of an electromechanical transducer.

$$e = Z_e i + T_{em} v \tag{11}$$

$$f = T_{me} i + Z_m v \tag{12}$$

where e is the Laplace transform of the input voltage across the electrical terminals, i the input current, f the force applied to the mechanical terminals, and v the velocity of the mechanical part. Z_e is the blocked electrical impedance, measured for $v = 0$; T_{em} is the transduction coefficient representing the electromotive force (voltage) appearing in the electrical circuit per unit velocity in the mechanical part (in *volt.sec/m*). T_{me} is the transduction coefficient representing the force acting on the mechanical terminals to balance the electromagnetic force induced per unit current input on the electrical side (in *N/Amp*), and Z_m is the mechanical impedance, measured when the electrical side is open ($i = 0$).

To illustrate this representation, consider the proof-mass actuator with the voltage source of Fig.4; the electrical equation reads

$$E(t) = Ri + L\frac{di}{dt} + Tv$$

or in Laplace form

$$E = (Ls + R)i + Tv$$

If F is the external force applied to the mechanical terminal (positive in the positive direction of v), the mechanical equation reads

$$F(t) = m\ddot{x} + c\dot{x} + kx - Ti$$

or in Laplace form (using the velocity as mechanical variable)

$$F = (ms + c + k/s)v - Ti$$

Thus, the constitutive equations may be written in the form (11) and (12) with

$$Z_e = Ls + R, \qquad Z_m = ms + c + k/s, \qquad T_{em} = T, \qquad T_{me} = -T$$

In absence of external force ($f = 0$), v can be resolved from Equ.(12) and substituted into Equ.(11), leading to

$$e = (Z_e - \frac{T_{em}T_{me}}{Z_m})i$$

$-T_{em}T_{me}/Z_m$ is called the *motional impedance*. The total driving point electrical impedance is the sum of the blocked and the motional impedances.

3.2 Self-sensing

Equation (11) shows that the voltage drop across the electrical terminals of any electromechanical transducer is the sum of a contribution proportional to the current applied and a contribution proportional to the velocity of the mechanical terminals. Thus, if $Z_e i$ can be measured and subtracted from e, a signal proportional to the velocity is obtained. This suggests the bridge structure of Fig.7. The bridge equations are as follows: for the branch containing the transducer,

$$e = Z_e I + T_{em} v + Z_b I$$

$$I = \frac{1}{Z_e + Z_b}(e - T_{em} v)$$

$$V_4 = Z_b I = \frac{Z_b}{Z_e + Z_b}(e - T_{em} v)$$

For the other branch,

$$e = kZ_e i + kZ_b i$$

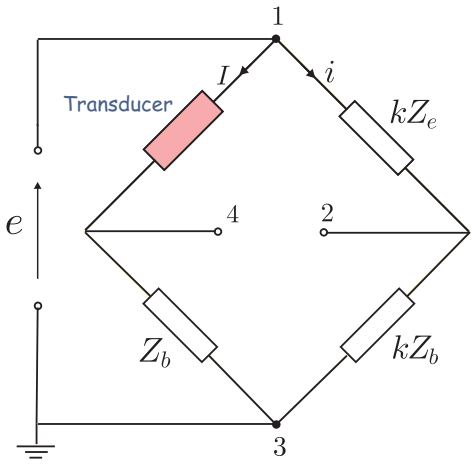

Figure 7. Bridge circuit for self-sensing actuation.

$$V_2 = kZ_b i = \frac{Z_b}{Z_e + Z_b}\, e$$

and the bridge output

$$V_4 - V_2 = \left(\frac{-Z_b\, T_{em}}{Z_e + Z_b}\right) v \tag{13}$$

is indeed a linear function of the velocity v of the mechanical terminals. Note, however, that $-Z_b\, T_{em}/(Z_e+Z_b)$ acts as a filter; the bridge impedance Z_b must be adapted to the transducer impedance Z_e to avoid amplitude distortion and phase shift between the output voltage $V_4 - V_2$ and the transducer velocity in the frequency band of interest.

4 Smart materials

Piezoelectric materials belong to the so-called *smart materials*, or *multifunctional materials*, which have the ability to respond significantly to stimuli of different physical natures. Figure 8 lists various effects that are observed in materials in response to various inputs: mechanical, electrical, magnetic, thermal, light. The coupling between the physical fields of different types is expressed by the non-diagonal cells in the figure; if its magnitude is sufficient, the coupling can be used to build discrete or distributed transducers of various types, which can be used as sensors, actuators, or even integrated in structures with various degrees of tailoring and complexity

Output / Input	Strain	Electric charge	Magnetic flux	Temperature	Light
Stress	Elasticity	Piezo-electricity	Magneto-striction		Photo-elasticity
Electric field	Piezo-electricity	Permittivity			Electro -optic effect
Magnetic field	Magneto-striction	Magneto-electric effect	Permeability		Magneto -optic
Heat	Thermal expansion	Pyro-electricity		Specific heat	
Light	Photostriction	Photo-voltaic effect			Refractive index

Figure 8. Stimulus-response relations indicating various effects in materials. The smart materials correspond to the non-diagonal cells.

(e.g. as fibers), to make them controllable or responsive to their environment (e.g. for shape morphing, precision shape control, damage detection, dynamic response alleviation,...).

Figure 9 summarizes the mechanical properties of a few smart materials which are considered for actuation in structural control applications. Figure 9.a shows the maximum (blocked) stress versus the maximum (free) strain; the diagonal lines in the diagram indicate a constant energy density. Figure 9.b shows the specific energy density (i.e. energy density by unit mass) versus the maximum frequency; the diagonal lines indicate a constant specific power density. Note that all the material characteristics vary by several orders of magnitude. Among them all, the piezoelectric materials are undoubtedly the most mature and those with the most applications.

5 Piezoelectric transducer

The piezoelectric effect was discovered by Pierre and Jacques Curie in 1880. The direct piezoelectric effect consists in the ability of certain crystalline materials to generate an electrical charge in proportion to an externally applied force; the direct effect is used in force transducers. According to

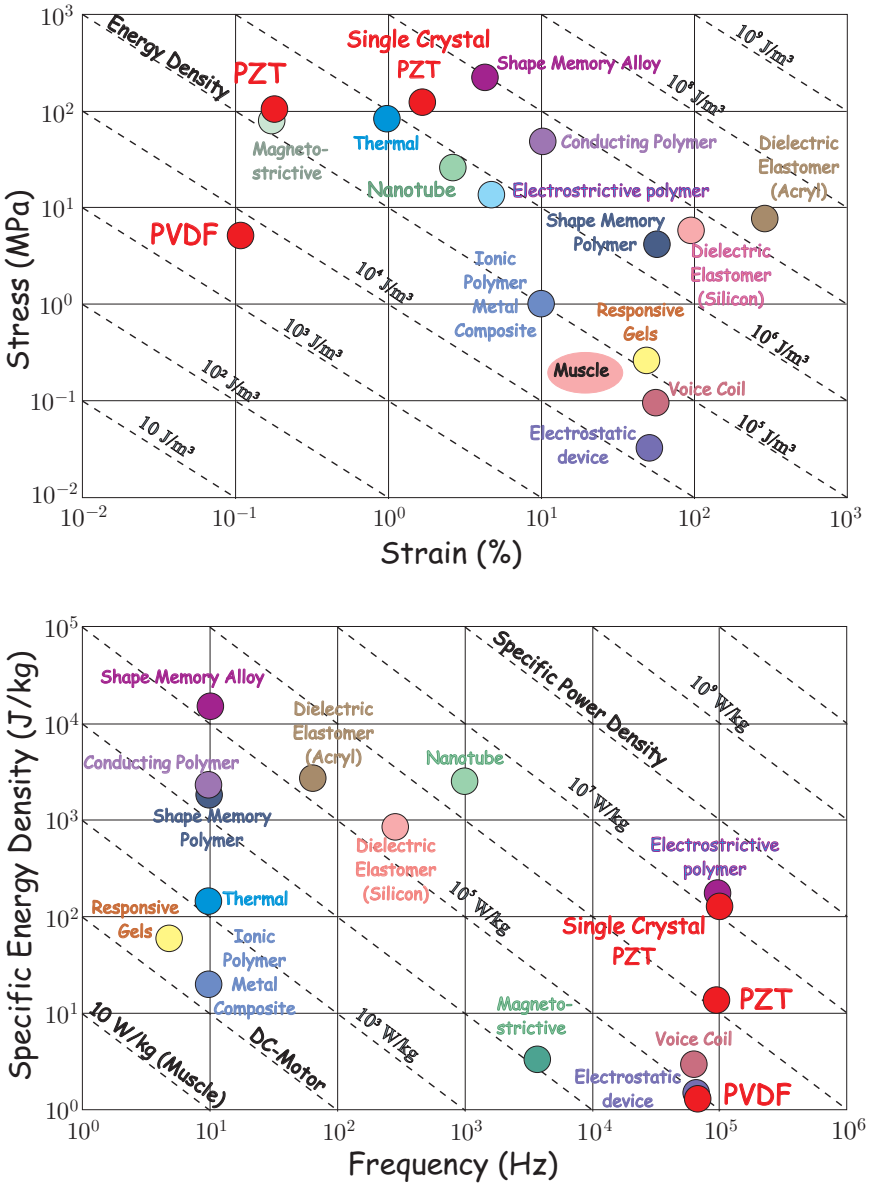

Figure 9. (a) Maximum stress vs. maximum strain of various smart material actuators. (b) Specific energy density vs. maximum frequency (by courtesy of R.Petricevic, *Neue Materialen Würzburg*).

the inverse piezoelectric effect, an electric field parallel to the direction of polarization induces an expansion of the material. The piezoelectric effect is anisotropic; it can be exhibited only by materials whose crystal structure has no center of symmetry; this is the case for some ceramics below a certain temperature called the *Curie temperature*; in this phase, the crystal has built-in electric dipoles, but the dipoles are randomly orientated and the net electric dipole on a macroscopic scale is zero. During the poling process, when the crystal is cooled in the presence of a high electric field, the dipoles tend to align, leading to an electric dipole on a macroscopic scale. After cooling and removing of the poling field, the dipoles cannot return to their original position; they remain aligned along the poling direction and the material body becomes permanently piezoelectric, with the ability to convert mechanical energy to electrical energy and vice versa; this property will be lost if the temperature exceeds the Curie temperature or if the transducer is subjected to an excessive electric field in the direction opposed to the poling field.

The most popular piezoelectric materials are *Lead-Zirconate-Titanate (PZT)* which is a ceramic, and *Polyvinylidene fluoride (PVDF)* which is a polymer. In addition to the piezoelectric effect, piezoelectric materials exhibit a *pyroelectric* effect, according to which electric charges are generated when the material is subjected to temperature; this effect is used to produce heat detectors; it will not be discussed here.

In this section, we consider a transducer made of a one-dimensional piezoelectric material of constitutive equations (we use the notations of the IEEE Standard on Piezoelectricity)

$$D = \varepsilon^T E + d_{33} T \tag{14}$$

$$S = d_{33} E + s^E T \tag{15}$$

where D is the electric displacement (charge per unit area, expressed in $Coulomb/m^2$), E the electric field (V/m), T the stress (N/m^2) and S the strain. ε^T is the dielectric constant (permittivity) under constant stress, s^E is the compliance when the electric field is constant (inverse of the Young's modulus) and d_{33} is the piezoelectric constant, expressed in m/V or $Coulomb/Newton$; the reason for the subscript 33 is that, by convention, index 3 is always aligned to the poling direction of the material, and we assume that the electric field is parallel to the poling direction. Note that the same constant d_{33} appears in (14) and (15).

In the absence of an external force, a transducer subjected to a voltage with the same polarity as that during poling produces an elongation, and a voltage opposed to that during poling makes it shrink (inverse piezoelectric effect). In (15), this amounts to a positive d_{33}. Conversely (direct piezoelectric effect), if we consider a transducer with open electrodes ($D = 0$), according to (14), $E = -(d_{33}/\varepsilon^T)T$, which means that a traction stress will produce a voltage with polarity opposed to that during poling, and a compressive stress will produce a voltage with the same polarity as that during poling.

5.1 Constitutive relations of a discrete transducer

Equations (14) and (15) can be written in a matrix form

$$\left\{ \begin{array}{c} D \\ S \end{array} \right\} = \left[\begin{array}{cc} \varepsilon^T & d_{33} \\ d_{33} & s^E \end{array} \right] \left\{ \begin{array}{c} E \\ T \end{array} \right\} \tag{16}$$

where (E, T) are the independent variables and (D, S) are the dependent variables. If (E, S) are taken as the independent variables, they can be rewritten

$$D = \frac{d_{33}}{s^E} S + \varepsilon^T \left(1 - \frac{{d_{33}}^2}{s^E \varepsilon^T} \right) E$$

$$T = \frac{1}{s^E} S - \frac{d_{33}}{s^E} E$$

or

$$\left\{ \begin{array}{c} D \\ T \end{array} \right\} = \left[\begin{array}{cc} \varepsilon^T (1 - k^2) & e_{33} \\ -e_{33} & c^E \end{array} \right] \left\{ \begin{array}{c} E \\ S \end{array} \right\} \tag{17}$$

where $c^E = 1/s^E$ is the Young's modulus under $E = 0$ (short circuited electrodes), in N/m^2 (Pa); $e_{33} = d_{33}/s^E$, the product of d_{33} by the Young modulus, is the constant relating the electric displacement to the strain for short-circuited electrodes (in $Coulomb/m^2$), and also that relating the compressive stress to the electric field when the transducer is blocked ($S = 0$).

$$k^2 = \frac{{d_{33}}^2}{s^E \varepsilon^T} = \frac{{e_{33}}^2}{c^E \varepsilon^T} \tag{18}$$

k is called the *Electromechanical coupling factor* of the material; it measures the efficiency of the conversion of mechanical energy into electrical energy, and vice versa, as discussed below. From (17), we note that $\varepsilon^T(1 - k^2)$ is the dielectric constant under zero strain.

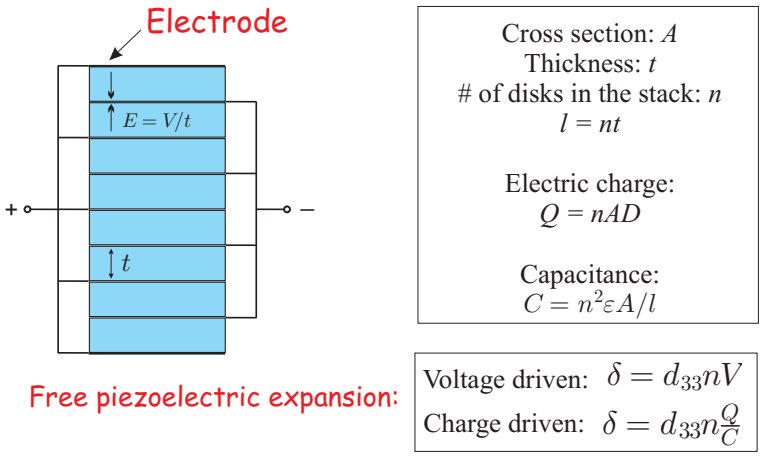

Figure 10. Piezoelectric linear transducer.

If one assumes that all the electrical and mechanical quantities are uniformly distributed in a linear transducer formed by a stack of n disks of thickness t and cross section A (Fig.9), the global constitutive equations of the transducer are obtained by integrating Equ.(16) or (17) over the volume of the transducer; one finds

$$\left\{ \begin{array}{c} Q \\ \Delta \end{array} \right\} = \left[\begin{array}{cc} C & nd_{33} \\ nd_{33} & 1/K_a \end{array} \right] \left\{ \begin{array}{c} V \\ f \end{array} \right\} \tag{19}$$

or

$$\left\{ \begin{array}{c} Q \\ f \end{array} \right\} = \left[\begin{array}{cc} C(1-k^2) & nd_{33}K_a \\ -nd_{33}K_a & K_a \end{array} \right] \left\{ \begin{array}{c} V \\ \Delta \end{array} \right\} \tag{20}$$

where $Q = nAD$ is the total electric charge on the electrodes of the transducer, $\Delta = Sl$ is the total extension ($l = nt$ is the length of the transducer), $f = AT$ is the total force and V the voltage applied between the electrodes of the transducer, resulting in an electric field $E = V/t = nV/l$. $C = \varepsilon^T An^2/l$ is the capacitance of the transducer with no external load ($f = 0$), $K_a = A/s^E l$ is the stiffness with short-circuited electrodes ($V = 0$). Note that the electromechanical coupling factor can be written alternatively

$$k^2 = \frac{{d_{33}}^2}{s^E \varepsilon^T} = \frac{n^2 {d_{33}}^2 K_a}{C} \tag{21}$$

Equation (19) can be inverted

$$\left\{ \begin{array}{c} V \\ f \end{array} \right\} = \frac{K_a}{C(1-k^2)} \left[\begin{array}{cc} 1/K_a & -nd_{33} \\ -nd_{33} & C \end{array} \right] \left\{ \begin{array}{c} Q \\ \Delta \end{array} \right\} \tag{22}$$

from which we can see that the stiffness with open electrodes ($Q = 0$) is $K_a/(1-k^2)$ and the capacitance for a fixed geometry ($\Delta = 0$) is $C(1-k^2)$. Note that typical values of k are in the range $0.3 - 0.7$; for large k, the stiffness changes significantly with the electrical boundary conditions, and similarly the capacitance depends on the mechanical boundary conditions.

Next, let us write the total stored electromechanical energy and coenergy functions.[1] Consider the discrete piezoelectric transducer of Fig.11; the

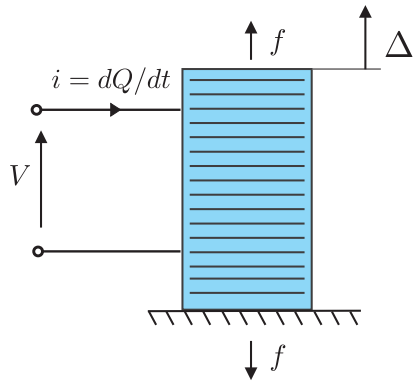

Figure 11. Discrete Piezoelectric transducer.

total power delivered to the transducer is the sum of the electric power, Vi and the mechanical power, $f\dot{\Delta}$. The net work on the transducer is

$$dW = Vidt + f\dot{\Delta}dt = VdQ + fd\Delta \tag{23}$$

For a conservative element, this work is converted into stored energy, dW_e, and the total stored energy, $W_e(\Delta, Q)$ can be obtained by integrating (23) from the reference state to the state (Δ, Q).[2] Upon differentiating $W_e(\Delta, Q)$,

$$dW_e(\Delta, Q) = \frac{\partial W_e}{\partial \Delta} d\Delta + \frac{\partial W_e}{\partial Q} dQ \tag{24}$$

[1] Energy and coenergy functions are needed in connection with energy formulations such as Hamilton principle, Lagrange equations or finite elements.

[2] Since the system is conservative, the integration can be done along any path leading from $(0, 0)$ to (Δ, Q).

and, comparing with (23), we recover the constitutive equations

$$f = \frac{\partial W_e}{\partial \Delta} \qquad\qquad V = \frac{\partial W_e}{\partial Q} \tag{25}$$

Substituting f and V from (22) into (23), one gets

$$dW_e = V dQ + f d\Delta$$

$$= \frac{Q\, dQ}{C(1-k^2)} - \frac{n d_{33} K_a}{C(1-k^2)}(\Delta\, dQ + Q\, d\Delta) + \frac{K_a}{1-k^2}\Delta\, d\Delta$$

which is the total differential of

$$W_e(\Delta, Q) = \frac{Q^2}{2C(1-k^2)} - \frac{n d_{33} K_a}{C(1-k^2)} Q\Delta + \frac{K_a}{1-k^2}\frac{\Delta^2}{2} \tag{26}$$

This is the analytical expression of the stored electromechanical energy for the discrete piezoelectric transducer. The partial derivatives (25) allow to recover the constitutive equations (22). The first term on the right hand side of (26) is the electrical energy stored in the capacitance $C(1-k^2)$ (corresponding to a fixed geometry, $\triangle = 0$); the third term is the elastic strain energy stored in a spring of stiffness $K_a/(1-k^2)$ (corresponding to open electrodes, $Q = 0$); the second term is the piezoelectric energy.

The electromechanical energy function uses Δ and Q as independent state variables. A *coenergy* function using Δ and V as independent variables can be defined by the *Legendre transformation*

$$W_e^*(\Delta, V) = VQ - W_e(\Delta, Q) \tag{27}$$

The total differential of the coenergy is

$$dW_e^* = Q\, dV + V\, dQ - \frac{\partial W_e}{\partial \Delta} d\Delta - \frac{\partial W_e}{\partial Q} dQ$$

$$dW_e^* = Q\, dV - f\, d\Delta \tag{28}$$

where Equ.(25) have been used. It follows that

$$Q = \frac{\partial W_e^*}{\partial V} \qquad \text{and} \qquad f = -\frac{\partial W_e^*}{\partial \Delta} \tag{29}$$

Introducing the constitutive equations (20) into (28),

$$dW_e^* = \left[C(1-k^2)V + n d_{33} K_a \Delta\right] dV + (n d_{33} K_a V - K_a \Delta)\, d\Delta$$

$$= C(1-k^2) V dV + n d_{33} K_a\, (\Delta dV + V d\Delta) - K_a \Delta\, d\Delta$$

which is the total differential of

$$W_e^*(\Delta, V) = C(1-k^2)\frac{V^2}{2} + nd_{33}K_aV\Delta - K_a\frac{\Delta^2}{2} \tag{30}$$

This is the analytical form of the coenergy function for the discrete piezoelectric transducer. The first term on the right hand side of (30) is recognized as the electrical coenergy in the capacitance $C(1-k^2)$ (corresponding to a fixed geometry, $\Delta = 0$); the third is the strain energy stored in a spring of stiffness K_a (corresponding to short-circuited electrodes, $V = 0$). The second term of (30) is the piezoelectric coenergy; using the fact that the uniform electric field is $E = nV/l$ and the uniform strain is $S = \Delta/l$, it can be rewritten

$$\int_\Omega Se_{33}E\, d\Omega \tag{31}$$

where the integral extends to the volume Ω of the transducer.

The analytical form (26) of the electromechanical energy, together with the constitutive equations (25) can be regarded as an alternative definition of a discrete piezoelectric transducer, and similarly for the analytical expression of the coenergy (30) and the constitutive equations (29).

5.2 Interpretation of k^2

Consider a piezoelectric transducer subjected to the following mechanical cycle: first, it is loaded with a force F with short-circuited electrodes; the resulting extension is

$$\Delta_1 = \frac{F}{K_a}$$

where $K_a = A/(s^E l)$ is the stiffness with short-circuited electrodes. The energy stored in the system is

$$W_1 = \int_0^{\Delta_1} f\, dx = \frac{F\Delta_1}{2} = \frac{F^2}{2K_a}$$

At this point, the electrodes are open and the transducer is unloaded according to a path of slope $K_a/(1-k^2)$, corresponding to the new electrical boundary conditions,

$$\Delta_2 = \frac{F(1-k^2)}{K_a}$$

The energy recovered in this way is

$$W_2 = \int_0^{\Delta_2} f\, dx = \frac{F\Delta_2}{2} = \frac{F^2(1-k^2)}{2K_a}$$

leaving $W_1 - W_2$ stored in the transducer. The ratio between the remaining stored energy and the initial stored energy is

$$\frac{W_1 - W_2}{W_1} = k^2$$

Similarly, consider the following electrical cycle: first, a voltage V is applied to the transducer which is mechanically unconstrained ($f = 0$). The electric charges appearing on the electrodes are

$$Q_1 = CV$$

where $C = \varepsilon^T An^2/l$ is the unconstrained capacitance, and the energy stored in the transducer is

$$W_1 = \int_0^{Q_1} v\, dq = \frac{VQ_1}{2} = \frac{CV^2}{2}$$

At this point, the transducer is blocked mechanically [changing its capacitance from C to $C(1 - k^2)$] and electrically unloaded from V to 0. The electrical charges are removed according to

$$Q_2 = C(1 - k^2)V$$

The energy recovered in this way is

$$W_2 = \int_0^{Q_2} v\, dq = \frac{C(1 - k^2)V^2}{2}$$

leaving $W_1 - W_2$ stored in the transducer. Here again, the ratio between the remaining stored energy and the initial stored energy is

$$\frac{W_1 - W_2}{W_1} = k^2$$

Although the foregoing relationships provide a clear physical interpretation of the electromechanical coupling factor, they do not bring a practical way of measuring k^2; the experimental determination of k^2 is often based on impedance (or admittance) measurements.

5.3 Admittance of the piezoelectric transducer

Consider the system of Fig.12, where the piezoelectric transducer is assumed massless and is connected to a mass M. The force acting on the mass is the negative of that acting on the transducer, $f = -M\ddot{x}$; using (20),

$$\left\{ \begin{array}{c} Q \\ -M\ddot{x} \end{array} \right\} = \left[\begin{array}{cc} C(1 - k^2) & nd_{33}K_a \\ -nd_{33}K_a & K_a \end{array} \right] \left\{ \begin{array}{c} V \\ x \end{array} \right\} \tag{32}$$

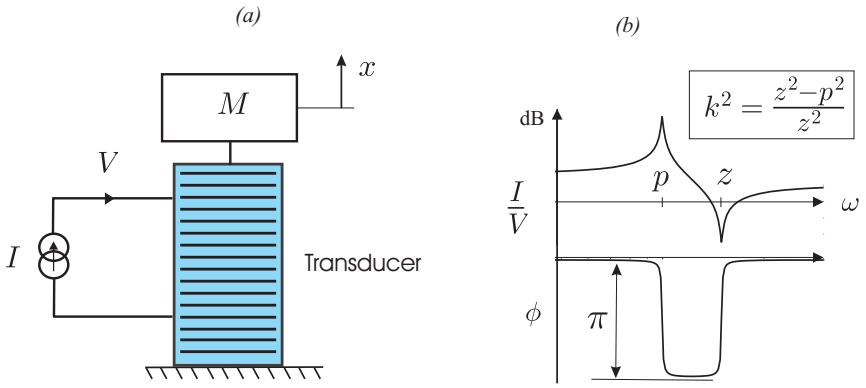

Figure 12. (a) Elementary dynamical model of the piezoelectric transducer. (b) Typical admittance FRF of the transducer, in the vicinity of its natural frequency.

From the second equation, one gets (in Laplace form)

$$x = \frac{nd_{33}K_a}{Ms^2 + K_a} V$$

and, substituting in the first one and using (21), one finds

$$\frac{Q}{V} = C(1-k^2)\left[\frac{Ms^2 + K_a/(1-k^2)}{Ms^2 + K_a}\right] \tag{33}$$

It follows that the admittance reads:

$$\frac{I}{V} = \frac{sQ}{V} = sC(1-k^2)\frac{s^2+z^2}{s^2+p^2} \tag{34}$$

where the poles and zeros are respectively

$$p^2 = \frac{K_a}{M} \qquad \text{and} \qquad z^2 = \frac{K_a/(1-k^2)}{M} \tag{35}$$

p is the natural frequency with short-circuited electrodes ($V = 0$) and z is the natural frequency with open electrodes ($I = 0$). From the previous equation one sees that

$$\frac{z^2 - p^2}{z^2} = k^2 \tag{36}$$

This relationship constitutes a practical way of determining the electromechanical coupling factor: An impedance meter is used to measure the Frequency Response Function (FRF) of the admittance (or the impedance), on

which the position of the poles p and zeros z are identified and introduced in Equ.(36).

6 Vibration isolation with voice coil transducers

6.1 Viscous damping isolator

Consider the spring mass system of Fig.13. A voice coil connects the mass M to the moving support and a resistor R is connected to the electrical terminals of the voice coil. The governing equations are

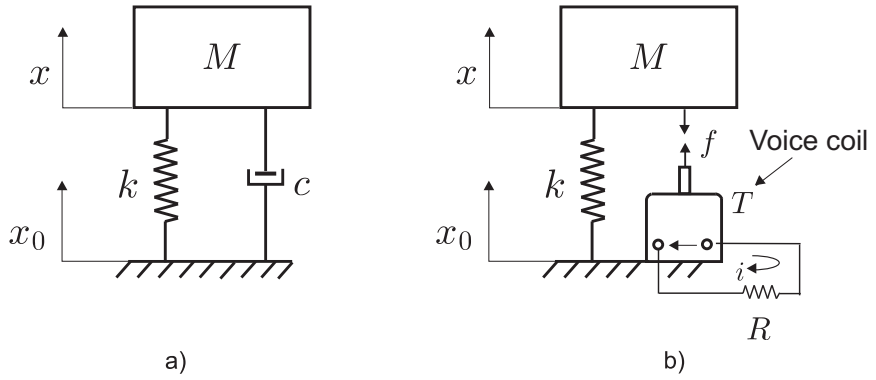

Figure 13. Voice coil used as viscous damper.

$$M\ddot{x} + k(x - x_0) = Ti$$

$$e = -Ri = Tv = T(\dot{x} - \dot{x}_0)$$

where the constitutive equations of the voice coil [Equ.(1) and (3)] have been used. Upon eliminating i between these equations, one finds

$$M\ddot{x} + \frac{T^2}{R}(\dot{x} - \dot{x}_0) + k(x - x_0) = 0 \tag{37}$$

Thus, when a resistor connects the electrical terminals of the voice coil, it behaves as a viscous damper of damping coefficient $c = T^2/R$; a lower resistance R will increase the damping (the minimum value of R is that of the coil itself). From the foregoing equation, the transmissibility of the isolator is readily obtained:

$$\frac{X}{X_0} = \frac{1 + 2j\xi\omega/\omega_n}{1 + 2j\xi\omega/\omega_n - \omega^2/\omega_n^2} \tag{38}$$

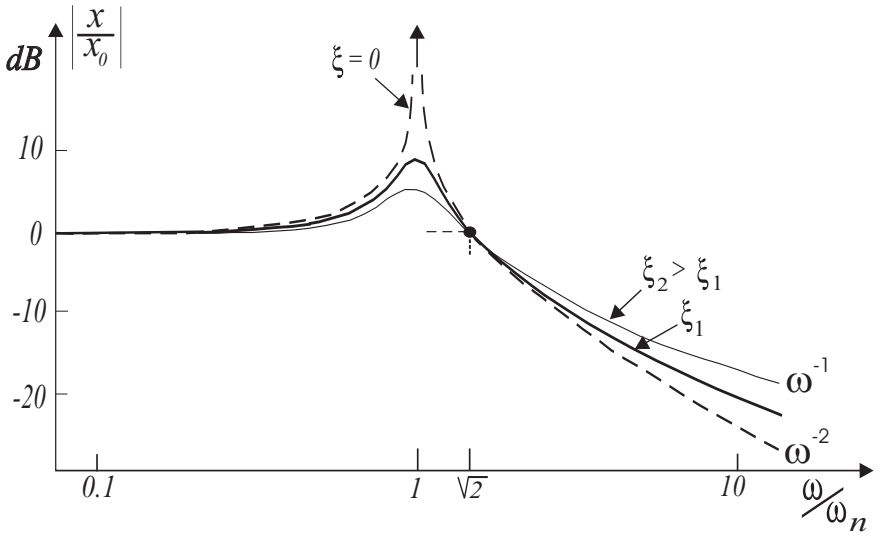

Figure 14. Transmissibility of the passive isolator for various values of the damping ratio ξ. The high frequency decay rate is ω^{-1}.

with the usual notations $\omega_n^2 = k/M$ and $2\xi\omega_n = c/M$. It is displayed in Fig.14 for various values of the damping ratio ξ: *(i)* All the curves are larger than 1 for $\omega < \sqrt{2}\ \omega_n$ and become smaller than 1 for $\omega > \sqrt{2}\ \omega_n$. Thus the critical frequency $\sqrt{2}\ \omega_n$ separates the domains of amplification and attenuation of the isolator. *(ii)* When $\xi = 0$, the high frequency decay rate is ω^{-2}, that is -40 *dB/decade*, while very large amplitudes occur near the corner frequency ω_n (the natural frequency of the spring-mass system).

Figure 14 illustrates the trade-off in passive isolator design: large damping is desirable at low frequency to reduce the resonant peak while low damping is needed at high frequency to maximize the isolation. One observes that if the disturbance is generated by a rotating unbalance of a motor with variable speed, there is an obvious benefit to use a damper with variable damping characteristics which can be adjusted according to the rotation velocity: high damping when $\omega < \sqrt{2}\omega_n$ and low damping when $\omega > \sqrt{2}\omega_n$. Such (*adaptive*) devices can be readily obtained with a variable resistor R. The following section discusses another electrical circuit which improves the high frequency decay rate of the isolator.

6.2 Relaxation isolator

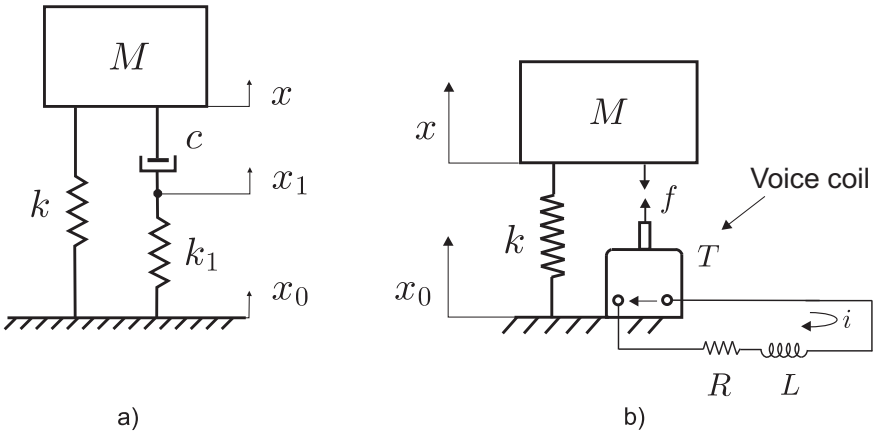

Figure 15. (a) Relaxation isolator. (b) Electromagnetic realization.

In the *relaxation* isolator, the viscous damper c is replaced by a Maxwell unit consisting of a damper c and a spring k_1 in series (Fig.15.a). The governing equations are

$$M\ddot{x} + k(x - x_0) + c(\dot{x} - \dot{x}_1) = 0 \tag{39}$$

$$c(\dot{x} - \dot{x}_1) = k_1(x_1 - x_0) \tag{40}$$

or, in matrix form using the Laplace variable s,

$$\begin{bmatrix} Ms^2 + cs + k & -cs \\ -cs & k_1 + cs \end{bmatrix} \begin{Bmatrix} x \\ x_1 \end{Bmatrix} = \begin{Bmatrix} k \\ k_1 \end{Bmatrix} x_0 \tag{41}$$

Upon inverting this system of equations, the transmissibility is obtained in Laplace form:

$$\frac{x}{x_0} = \frac{(k_1 + cs)k + k_1 cs}{(Ms^2 + cs + k)(k_1 + cs) - c^2 s^2} = \frac{(k_1 + cs)k + k_1 cs}{(Ms^2 + k)(k_1 + cs) + k_1 cs} \tag{42}$$

One sees that the asymptotic decay[3] rate for large frequencies is in s^{-2}, that is -40 *dB/decade*. Physically, this corresponds to the fact that, at high

[3] the asymptotic decay rate is governed by the largest power of s of the numerator and the denominator.

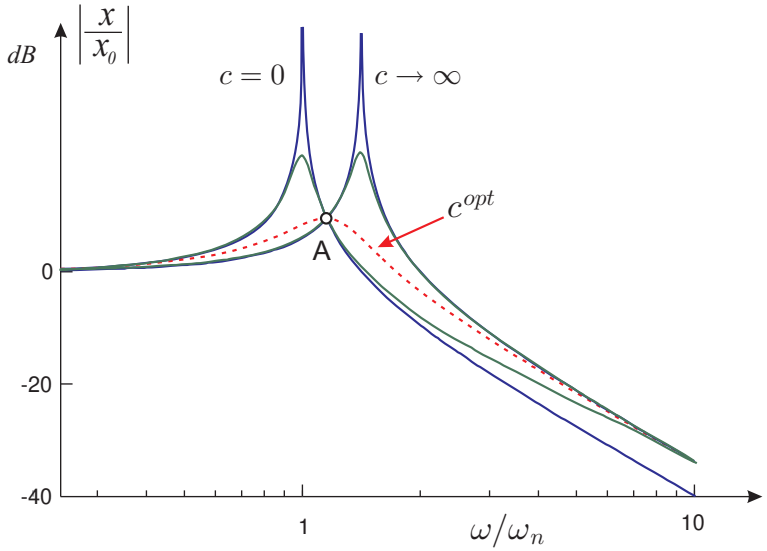

Figure 16. Transmissibility of the relaxation oscillator for fixed values of k and k_1 and various values of c. The first peak corresponds to $\omega = \omega_n = (k/M)^{1/2}$; the second one corresponds to $\omega = \Omega_n = [(k + k_1)/M]^{1/2}$. All the curves cross each other at A and have an asymptotic decay rate of -40 *dB/decade*. The curve corresponding to c_{opt} is nearly maximum at A.

frequency, the viscous damper tends to be blocked, and the system behaves like an undamped isolator with two springs acting in parallel. Figure 16 compares the transmissibility curves for given values of k and k_1 and various values of c. For $c = 0$, the relaxation isolator behaves like an undamped isolator of natural frequency $\omega_n = (k/M)^{1/2}$. Likewise, for $c \to \infty$, it behaves like an undamped isolator of frequency $\Omega_n = [(k + k_1)/M]^{1/2}$. In between, the poles of the system are solution of the characteristic equation

$$(Ms^2 + k)(k_1 + cs) + k_1 cs = (Ms^2 + k)k_1 + cs(Ms^2 + k + k_1) = 0$$

which can be rewritten in root locus form

$$1 + \frac{k_1}{c} \frac{s^2 + \omega_n^2}{s(s^2 + \Omega_n^2)} = 0 \tag{43}$$

It is represented in Fig.17 when c varies from 0 to ∞; it can be shown that

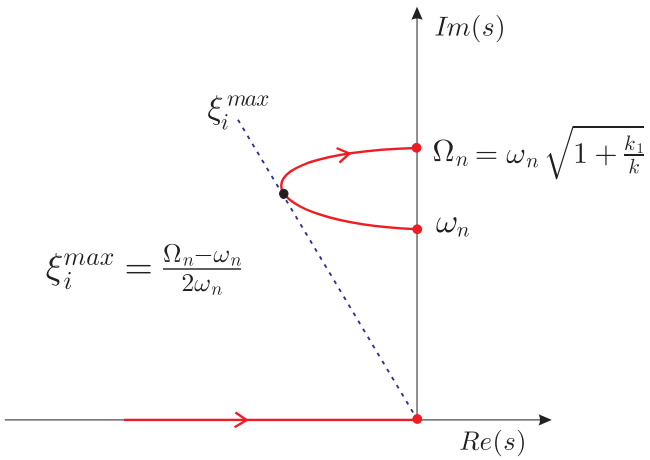

Figure 17. Root locus of the solutions of Equ.(43) as c goes from zero to infinity. The maximum damping is achieved for $k_1/c = \Omega_n^{3/2}\omega_n^{-1/2}$.

the maximum damping ratio is achieved for

$$\frac{k_1}{c} = \frac{\Omega_n^{3/2}}{\omega_n^{1/2}} \tag{44}$$

and the corresponding damper constant is

$$c_{opt} = \frac{k_1}{\Omega_n}(\frac{\omega_n}{\Omega_n})^{1/2} = \frac{k_1}{\Omega_n}(1+\frac{k_1}{k})^{-1/4} = \frac{k_1}{\omega_n}(1+\frac{k_1}{k})^{-3/4} \tag{45}$$

The transmissibility corresponding to c_{opt} is also represented in Fig.16; it is nearly maximum at A.

Electromagnetic realization The principle of the relaxation isolator is simple and it can be realized with viscoelastic materials. However, it may be difficult to integrate in the system, and also viscoelastic materials are notorious for their thermal sensitivity. In some circumstances, especially when thermal stability is critical, it may be more convenient to achieve the same effect through a voice coil transducer whose electrical terminals are connected to an inductor L and a resistor R (Fig.15.b). The governing equations of the system are in this case

$$M\ddot{x} + k(x - x_0) - Ti = 0 \tag{46}$$

$$L\frac{di}{dt} + T(\dot{x} - \dot{x}_0) + Ri = 0 \tag{47}$$

where T is the transducer constant. In matrix form, using the Laplace variable,

$$\begin{bmatrix} Ms^2 + k & -T \\ Ts & Ls + R \end{bmatrix} \begin{Bmatrix} x \\ i \end{Bmatrix} = \begin{Bmatrix} k \\ Ts \end{Bmatrix} x_0 \tag{48}$$

It follows that the transmissibility reads

$$\frac{x}{x_0} = \frac{(Ls + R)k + T^2 s}{(Ms^2 + k)(Ls + R) + T^2 s} \tag{49}$$

Comparing with Equ.(42), one sees that the electromechanical isolator behaves exactly like a relaxation isolator provided that

$$\frac{Ls + R}{T^2} = \frac{cs + k_1}{k_1 c} \tag{50}$$

or

$$k_1 = \frac{T^2}{L} \qquad c = \frac{T^2}{R} \tag{51}$$

These are the two relationships between the three parameters T, L and R so that the transmissibility of the electromechanical system of Fig.15.b is the same as that of Fig.15.a.

7 Controlling structures with piezo transducers

Consider a structure with a single discrete piezoelectric transducer (Fig.18); the transducer is governed by Equ.(20):

$$\begin{Bmatrix} Q \\ f \end{Bmatrix} = \begin{bmatrix} C(1 - k^2) & nd_{33}K_a \\ -nd_{33}K_a & K_a \end{bmatrix} \begin{Bmatrix} V \\ b^T x \end{Bmatrix} \tag{52}$$

where $\Delta = b^T x$ is the relative displacement at the extremities of the transducer. The dynamics of the structure is governed by

$$M\ddot{x} + K^* x = -bf \tag{53}$$

where K^* is the stiffness matrix of the structure without the transducer and b is the influence vector of the transducer in the global coordinate system of the structure. The non-zero components of b are the direction cosines of the active bar. The minus sign on the right hand side of the previous equation comes from the fact that the force acting on the structure is opposed to that acting on the transducer. Note that the same vector b appears in both

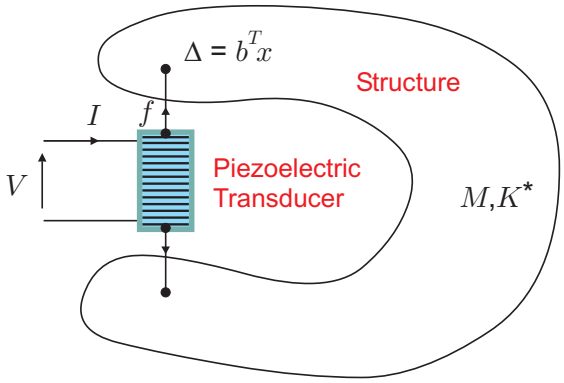

Figure 18. Structure with a piezoelectric transducer. b is the influence vector of the transducer in the global coordinate system of the structure.

equations because the relative displacement is measured along the direction of f. Substituting f from the constitutive equation into the second equation, one finds

$$M\ddot{x} + (K^* + bb^T K_a)x = b\, K_a n d_{33} V$$

or

$$M\ddot{x} + Kx = bK_a\delta \tag{54}$$

where $K = K^* + bb^T K_a$ is the global stiffness matrix of the structure including the piezoelectric transducer in short-circuited conditions (which contributes for $bb^T K_a$); $\delta = nd_{33}V$ is the *free expansion* of the transducer induced by a voltage V; $K_a\delta$ is the equivalent piezoelectric loading: the effect of the piezoelectric transducer on the structure consists of a pair of *self-equilibrating* forces applied axially to the ends of the transducer; as for thermal loads, their magnitude is equal to the product of the stiffness of the transducer (in short-circuited conditions) by the unconstrained piezoelectric expansion; this is known as the *thermal analogy*.

Let ϕ_i be the normal modes, solutions of the eigenvalue problem

$$(K - \omega_i^2 M)\phi_i = 0 \tag{55}$$

They satisfy the usual orthogonality conditions

$$\phi_i^T M \phi_j = \mu_i \delta_{ij} \tag{56}$$

$$\phi_i^T K \phi_j = \mu_i \omega_i^2 \delta_{ij} \tag{57}$$

where ω_i is the natural frequency when the transducer is short-circuited. If the global displacements are expanded into modal coordinates,

$$x = \sum_i z_i \phi_i \tag{58}$$

where z_i are the modal amplitudes, Equ.(54) is easily transformed into

$$\mu_i(\ddot{z}_i + \omega_i^2 z_i) = \phi_i^T b K_a \delta \tag{59}$$

Upon taking the Laplace transform, one easily gets

$$x = \sum_{i=1}^{n} \frac{\phi_i \phi_i^T}{\mu_i(\omega_i^2 + s^2)} b K_a \delta \tag{60}$$

and the transducer extension

$$\Delta = b^T x = \sum_{i=1}^{n} \frac{K_a (b^T \phi_i)^2}{\mu_i \omega_i^2 (1 + s^2/\omega_i^2)} \, \delta \tag{61}$$

From Equ.(57), $\mu_i \omega_i^2/2$ is clearly the strain energy in the structure when it vibrates according to mode i, and $K_a(b^T\phi_i)^2/2$ represents the strain energy in the transducer when the structure vibrates according to mode i. Thus, the ratio

$$\nu_i = \frac{K_a (b^T \phi_i)^2}{\mu_i \omega_i^2} \tag{62}$$

is readily interpreted as the *fraction of modal strain energy* in the transducer for mode i. With this notation, the previous equation is rewritten

$$\Delta = b^T x = \sum_{i=1}^{n} \frac{\nu_i}{(1 + s^2/\omega_i^2)} \, \delta \tag{63}$$

which relates the actual displacement of the transducer with the free expansion due to the voltage V.

7.1 Force feedback open-loop transfer function

A frequent control configuration is that of an active strut where the piezoelectric actuator is coupled with a collocated force sensor. From the second constitutive equation (52), the open-loop transfer function between the free expansion $\delta = n d_{33} V$ of the transducer (proportional to the applied voltage) and the output force f in the active strut is readily obtained:

$$f = -K_a \delta + K_a \Delta$$

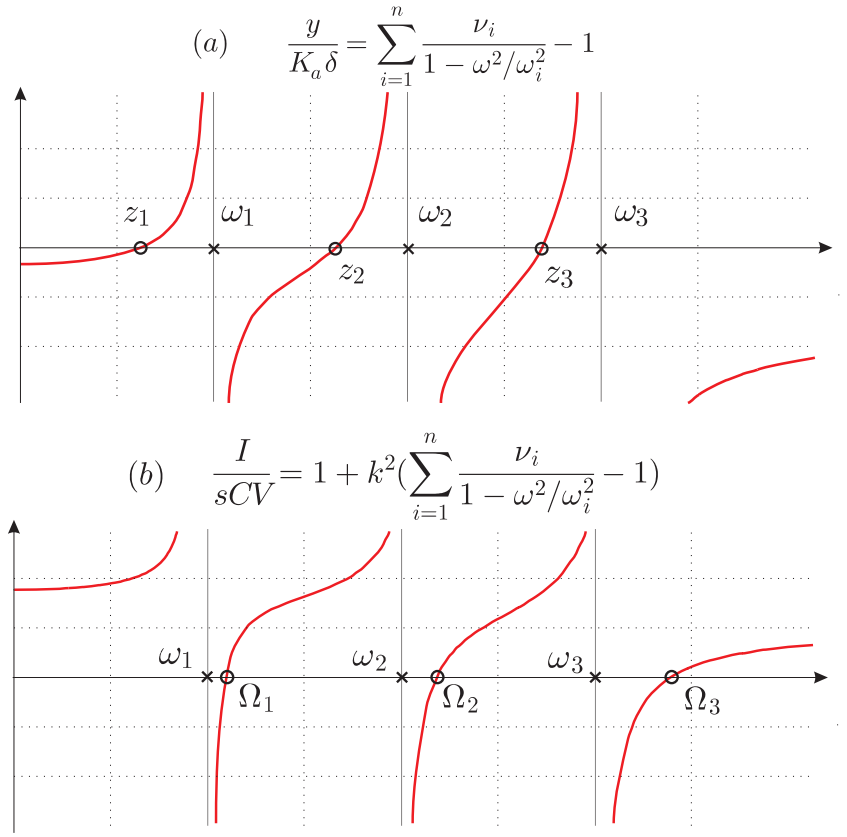

Figure 19. (a) Open-loop FRF of the active strut mounted in the structure (undamped). (b) Admittance of the transducer mounted in the structure; the poles are the natural frequencies with short-circuited electrodes ω_i and the zeros are the natural frequencies with open electrodes Ω_i.

or

$$\frac{f}{\delta} = K_a[\sum_{i=1}^{n} \frac{\nu_i}{(1+s^2/\omega_i^2)} - 1] \tag{64}$$

All the residues being positive, there will be alternating poles and zeros along the imaginary axis. Note the presence of a feedthrough in the transfer function. Figure 19.a shows the open-loop FRF in the undamped case; as expected the poles at $\pm j\omega_i$ are interlaced with the zeros at $\pm z_i$. The transfer function can be truncated after m modes, assuming that the modes above

a certain order m have no dynamic amplification:

$$\frac{f}{\delta} = K_a[\sum_{i=1}^{m} \frac{\nu_i}{(1+s^2/\omega_i^2)} + \sum_{i=m+1}^{n} \nu_i - 1] \tag{65}$$

Collocated force feedback can be used very efficiently for active damping of structures, using Integral Force Feedback (IFF) and its variants; this topic is discussed extensively in [Preumont, 2011].

7.2 Admittance function

According to the first constitutive equation (52),

$$Q = C(1-k^2)V + nd_{33}K_a b^T x$$

Using (63),

$$Q = C(1-k^2)V + n^2 d_{33}^2 K_a \sum_{i=1}^{n} \frac{\nu_i}{(1+s^2/\omega_i^2)} V \tag{66}$$

and, taking into account the definition (21) of the electromechanical coupling factor, one finds the dynamic capacitance

$$\frac{Q}{V} = C(1-k^2)[1 + \frac{k^2}{1-k^2} \sum_{i=1}^{n} \frac{\nu_i}{(1+s^2/\omega_i^2)}] \tag{67}$$

The admittance is related to the dynamic capacitance by $I/V = sQ/V$:

$$\frac{I}{V} = \frac{sQ}{V} = sC(1-k^2)[1 + \sum_{i=1}^{n} \frac{K_i^2}{(1+s^2/\omega_i^2)}] \tag{68}$$

where

$$K_i^2 = \frac{k^2 \nu_i}{1-k^2} \tag{69}$$

is the effective electromechanical coupling factor for mode i.[4] The corresponding FRF is represented in Fig.19.b. The zeros of the admittance (or the dynamic capacitance) function correspond to the natural frequencies Ω_i with open electrodes (ω_i is the natural frequency with short-circuited electrodes) and

$$K_i^2 \simeq \frac{\Omega_i^2 - \omega_i^2}{\omega_i^2} \tag{70}$$

[4]Note that k^2 is a material property while ν_i depends on the mode shape, the size and the location of the transducer inside the structure.

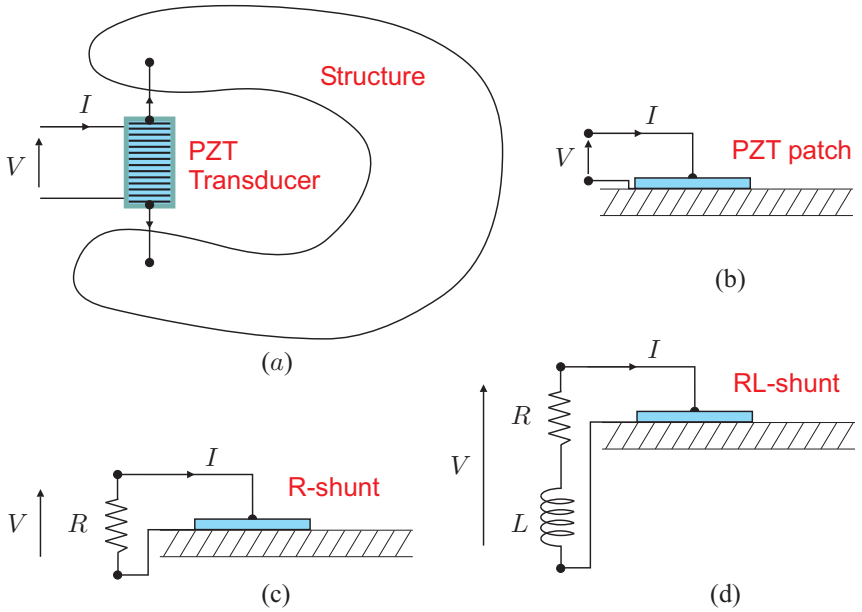

Figure 20. Structure with a piezoelectric transducer (a) in d_{33} mode (b) in d_{31} mode (c) R shunt (d) RL shunt.

The admittance of the transducer integrated in the structure may be written

$$\frac{I}{V} = sC_{\text{stat}}.\frac{\prod_{i=1}^{n}(1+s^2/\Omega_i^2)}{\prod_{j=1}^{n}(1+s^2/\omega_j^2)} \tag{71}$$

where C_{stat} is the static capacitance of the transducer when integrated in the structure; it lies between C and $C(1-k^2)$ depending on the restraint offered by the structure.

7.3 Passive damping with a piezoelectric transducer

It is possible to achieve passive damping by integrating piezoelectric transducers at proper locations in a structure and shunting them on passive electrical networks. The theory is explained here with the simple case of a discrete transducer, but more complicated configurations are possible (Fig.20).

Resistive shunting Using the same positive signs for V and I as for the structure (Fig.20.c), the voltage drop in the resistor is $V = -RI$; therefore, the admittance of the shunt is $-1/R$. The characteristic equation of the system is obtained by expressing the equality between the admittance of the structure and that of the passive shunt:

$$-\frac{1}{R} = sC(1-k^2)[1 + \sum_{i=1}^{n} \frac{K_i^2}{1+s^2/\omega_i^2}] \tag{72}$$

or

$$-\frac{1}{sRC(1-k^2)} = 1 + \sum_{i=1}^{n} \frac{K_i^2 \omega_i^2}{s^2+\omega_i^2} \tag{73}$$

In the vicinity of $\pm j\omega_i$, the sum is dominated by the contribution of mode i and the other terms can be neglected; defining $\gamma = [RC(1-k^2)]^{-1}$, the equation may be simplified as

$$-\frac{\gamma}{s} = 1 + \frac{K_i^2 \omega_i^2}{s^2+\omega_i^2}$$

which, using Equ.(70), can be rewritten

$$1 + \gamma \frac{s^2+\omega_i^2}{s(s^2+\Omega_i^2)} = 0 \tag{74}$$

This form of the characteristic equation is identical to Equ.(43) that we met earlier in this chapter. The root locus is represented in Fig.21; the parameter γ acts as the feedback gain in classical root locus plots. For $\gamma = 0$ ($R = \infty$), the poles are purely imaginary, $\pm j\Omega_i$, corresponding to the natural frequency of the system with open electrodes; the system is undamped. As the resistance decreases (γ increases), the poles move to the left and some damping appears in the system; it can be shown that the maximum damping is achieved for $\gamma = \Omega_i \sqrt{\Omega_i/\omega_i} \simeq \Omega_i$ and is

$$\xi_i^{\max} = \frac{\Omega_i - \omega_i}{2\omega_i} \simeq \frac{\Omega_i^2 - \omega_i^2}{4\omega_i^2} = \frac{K_i^2}{4} \tag{75}$$

Inductive shunting Since the electrical behavior of a piezoelectric transducer is essentially that of a capacitor, the idea with the RL shunt is to produce a RLC circuit which will be tuned on the natural frequency of the targeted mode and will act as a dynamic vibration absorber. We proceed in the same way as in the previous section, but with a RL-shunt (Fig.20.d); the admittance of the shunt is now $I/V = -1/(R+Ls)$. The characteristic

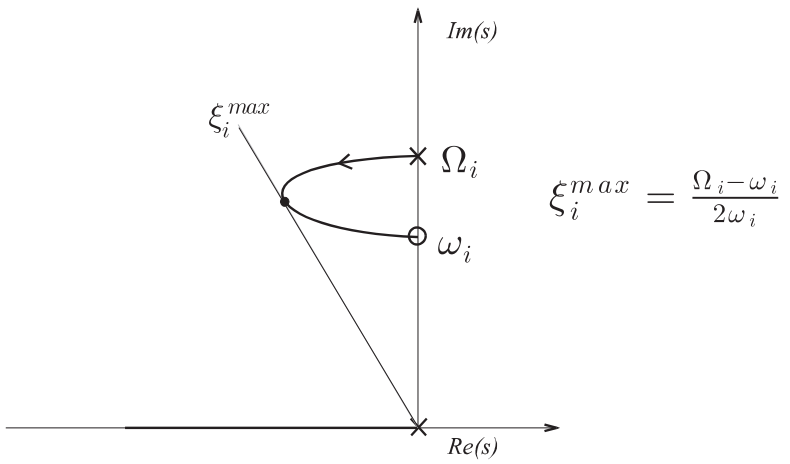

Figure 21. Resistive shunt. Evolution of the poles of the system as $\gamma = [RC(1-k^2)]^{-1}$ goes from 0 to ∞ (the diagram is symmetrical with respect to the real axis, only the upper half is shown).

equation is obtained by expressing the equality between the admittance of the structure and that of the passive shunt:

$$-\frac{1}{R+Ls} = sC(1-k^2)[1+\sum_{i=1}^{n}\frac{K_i^2}{1+s^2/\omega_i^2}] \tag{76}$$

or

$$-\frac{1}{(R+Ls)sC(1-k^2)} = 1+\sum_{i=1}^{n}\frac{K_i^2\omega_i^2}{s^2+\omega_i^2} \tag{77}$$

Once again, in the vicinity of $\pm j\omega_i$, the sum is dominated by the contribution of mode i and the equation is simplified as

$$-\frac{1}{(R+Ls)sC(1-k^2)} = 1+\frac{K_i^2\omega_i^2}{s^2+\omega_i^2} \tag{78}$$

Defining the electrical frequency

$$\omega_e^2 = \frac{1}{LC(1-k^2)} \tag{79}$$

and the electrical damping

$$2\xi_e\omega_e = \frac{R}{L} \tag{80}$$

Equ.(78) is rewritten

$$-\frac{\omega_e^2}{2\xi_e\omega_e s+s^2}=1+\frac{K_i^2\omega_i^2}{s^2+\omega_i^2}=\frac{s^2+\Omega_i^2}{s^2+\omega_i^2} \tag{81}$$

or

$$s^4+2\xi_e\omega_e s^3+(\Omega_i^2+\omega_e^2)s^2+2\Omega_i^2\xi_e\omega_e s+\omega_i^2\omega_e^2=0 \tag{82}$$

This can be rewritten in a root locus form

$$1+2\xi_e\omega_e\frac{s(s^2+\Omega_i^2)}{s^4+(\Omega_i^2+\omega_e^2)s^2+\omega_i^2\omega_e^2}=0 \tag{83}$$

In this formulation, $2\xi_e\omega_e = R/L$ plays the role of the gain in a classical root locus. Note that, for large R, the poles tend to $\pm j\Omega_i$, as expected. For $R = 0$ (i.e. $\xi_e = 0$), they are the solutions p_1 and p_2 of the characteristic equation $s^4+(\Omega_i^2+\omega_e^2)s^2+\omega_i^2\omega_e^2=0$ which accounts for the classical double peak of resonant dampers, with p_1 above $j\Omega_i$ and p_2 below $j\omega_i$. Figure 22 shows the root locus for a fixed value of ω_i/Ω_i and various values of the electrical tuning, expressed by the ratio

$$\alpha_e=\frac{\omega_e\omega_i}{\Omega_i^2} \tag{84}$$

The locus consists of two loops, starting respectively from p_1 and p_2; one of them goes to $j\Omega_i$ and the other goes to the real axis, near $-\Omega_i$. If $\alpha_e > 1$ (Fig.22.a), the upper loop starting from p_1 goes to the real axis, and that starting from p_2 goes to $j\Omega_i$, and the upper pole is always more heavily damped than the lower one (note that, if $\omega_e \to \infty$, $p_1 \to \infty$ and $p_2 \to j\omega_i$; the lower branch of the root locus becomes that of the resistive shunting). The opposite situation occurs if $\alpha_e < 1$ (Fig.22.b): the upper loop goes from p_1 to $j\Omega_i$ and the lower one goes from p_2 to the real axis; the lower pole is always more heavily damped. If $\alpha_e = 1$ (Fig.22.c), the two poles are always equally damped until the two branches touch each other in Q. This double root is achieved for

$$\alpha_e=\frac{\omega_e\omega_i}{\Omega_i^2}=1 \qquad , \qquad \xi_e^2=1-\frac{\omega_i^2}{\Omega_i^2}\simeq K_i^2 \tag{85}$$

This can be regarded as the optimum tuning of the inductive shunting. The corresponding eigenvalues satisfy

$$s^2+\Omega_i^2+\Omega_i(\frac{\Omega_i^2}{\omega_i^2}-1)^{1/2}s=0 \tag{86}$$

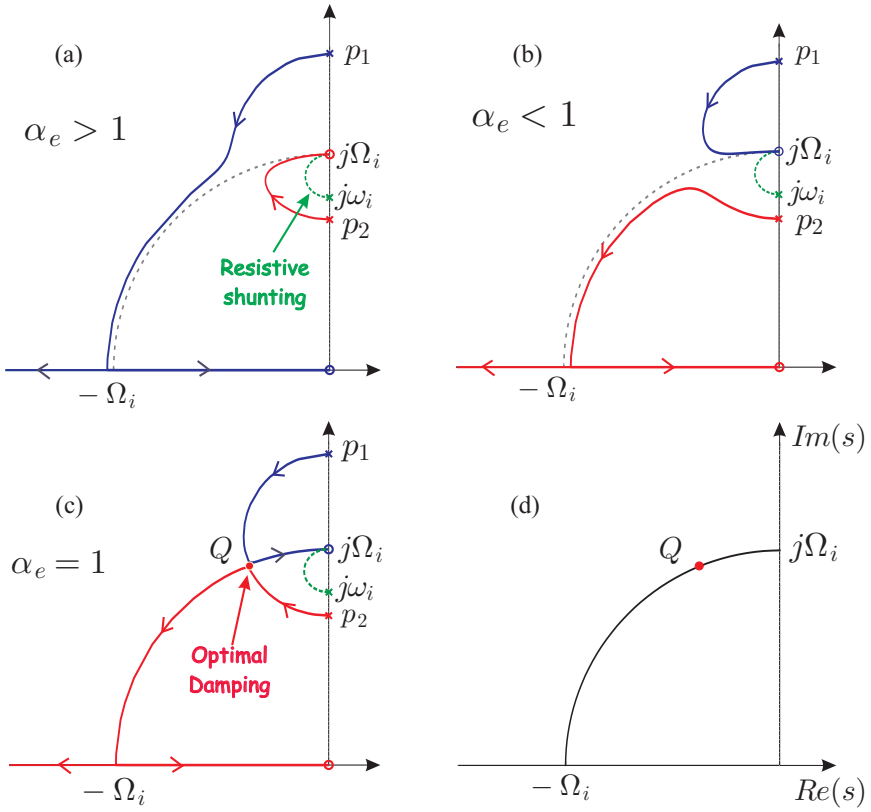

Figure 22. Root locus plot for inductive shunting (only the upper half is shown). The optimum damping at Q is achieved for $\alpha_e = 1$ and $\xi_e = K_i$; the maximum modal damping is $\xi_i \simeq K_i/2$.

For various values of ω_i/Ω_i (or K_i), the optimum poles at Q move along a circle of radius Ω_i (Fig.22.d). The corresponding damping ratio can be obtained easily by identifying the previous equation with the classical form of the damped oscillator, $s^2 + 2\xi_i\Omega_i s + \Omega_i^2 = 0$, leading to

$$\xi_i = \frac{1}{2}\left(\frac{\Omega_i^2}{\omega_i^2} - 1\right)^{1/2} = \frac{K_i}{2} = \frac{1}{2}\left(\frac{k^2\nu_i}{1-k^2}\right)^{1/2} \tag{87}$$

This value is significantly higher than that achieved with purely resistive shunting [it is exactly the square-root of (75)]. Note, however, that it is much more sensitive to the tuning of the electrical parameters on the tar-

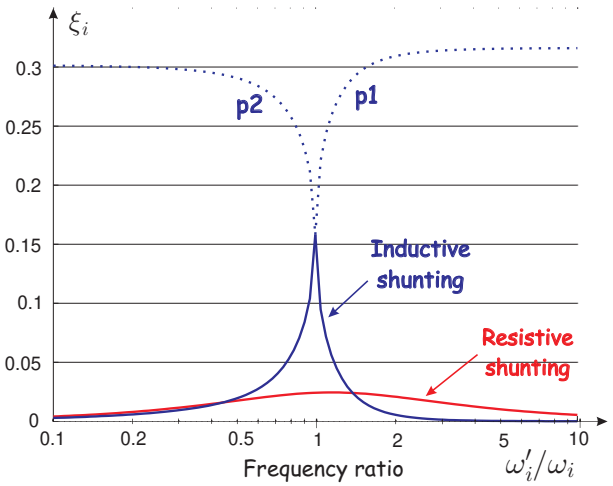

Figure 23. Evolution of the damping ratio of the inductive and resistive shunting with the de-tuning of the structural mode. ω_i is the natural frequency for which the shunt has been optimized, ω_i' is the actual value ($k = 0.5$, $\nu_i = 0.3$).

geted modes. This is illustrated in Fig.23, which displays the evolution of the damping ratio ξ_i when the actual natural frequency ω_i' moves away from the nominal frequency ω_i for which the shunt has been optimized (the damping ratio associated with p_1 and p_2 is plotted in dotted lines; the ratio ω_i'/Ω_i' is kept constant in all cases). One sees that the performance of the inductive shunting drops rapidly below that of the resistive shunting when the de-tuning increases. Note that, for low frequency modes, the optimum inductance value can be very large; such large inductors can be synthesized electronically. The multimodal passive damping via resonant shunt has been investigated by [Hollkamp, 1994].

Bibliography

CADY, W.G., *Piezoelectricity: an Introduction to the Theory and Applications of Electromechanical Phenomena in Crystals*, , McGrawHill, 1946.

CRANDALL, S.H., KARNOPP, D.C., KURTZ, E.F, Jr., PRIDMORE-BROWN, D.C. *Dynamics of Mechanical and Electromechanical Systems*, McGraw-Hill, N-Y, 1968.

DE BOER, E., Theory of Motional Feedback, *IRE Transactions on Audio*,

15-21, Jan.-Feb., 1961.

HOLTERMAN, J. & GROEN, P. *An Introduction to Piezoelectric Materials and Components*, Stichting Applied Piezo, 2012.

HOLLKAMP, J.J. Multimodal passive vibration suppression with piezoelectric materials and resonant shunts, *J. Intell. Material Syst. Structures*, Vol.5, Jan. 1994.

HUNT, F.V. *Electroacoustics: The Analysis of Transduction, and its Historical Background*, Harvard Monographs in Applied Science, No 5, 1954. Reprinted, Acoustical Society of America, 1982.

IEEE Standard on Piezoelectricity. (ANSI/IEEE Std 176-1987).

VAN RANDERAAT, J. & SETTERINGTON, R.E. (Edts) *Philips Application Book on Piezoelectric Ceramics*, Mullard Limited, London, 1974.

Physik Intrumente catalogue, Products for Micropositioning (*PI* GmbH).

PRATT, J., FLATAU, A. Development and analysis of self-sensing magnetostrictive actuator design, SPIE Smart Materials and Structures Conference, Vol.1917, 1993.

PREUMONT, A. *Vibration Control of Active Structures, An Introduction*, Third Edition, Springer, 2011.

PREUMONT, A. *Mechatronics, Dynamics of Electromechanical and Piezoelectric Systems*, Springer, 2006.

ROSEN, C.A. Ceramic transformers and filters, Proc. Electronic Component Symposium, p.205-211, 1956.

UCHINO, K. *Ferroelectric Devices*, Marcel Dekker, 2000.

WOODSON, H.H., MELCHER, J.R. *Electromechanical Dynamics, Part I: Discrete Systems*, Wiley, 1968.